

## Lack of Evidence for Orbital-Current Effects in the High-Temperature $Y_2Ba_4Cu_7O_{15-\delta}$ Superconductor using $^{89}Y$ Nuclear Magnetic Resonance

S. Strässle,\* J. Roos, M. Mali, and H. Keller

*Physik-Institut, Universität Zürich, CH-8057 Zürich, Switzerland*

T. Ohno

*Department of Physics, Faculty of Engineering, Tokushima University, Tokushima 770-8506, Japan*

(Received 7 May 2008; published 1 December 2008)

We have performed NMR measurements at the Y site on a *c*-axis-oriented powder sample of the cuprate superconductor  $Y_2Ba_4Cu_7O_{15-\delta}$  to search for the possible orbital-current phase. The temperature dependence of the Y linewidth and relaxation behavior in the normal-conducting phase were studied down to 100 K. These measurements give upper limits for a static magnetic field and the amplitude of a fluctuating magnetic field at the Y site of  $\approx 0.15$  and  $\approx 0.7$  mT, respectively. These values provide significant constraints on possible static or quasistatic orbital currents.

DOI: 10.1103/PhysRevLett.101.237001

PACS numbers: 74.25.Nf, 74.72.Bk, 75.40.Cx, 76.60.Jx

More than two decades after the discovery of high- $T_c$  superconductivity, the understanding of the underlying mechanism still remains a key issue. Significant progress in experimental techniques has been made with respect to the cuprate problem, enabling deep insight into the nature of the phenomenon. Many theories and ideas to capture the physics of these oxides have been suggested, but there is yet no consensus on a theory of high- $T_c$  superconductivity. Recent efforts [1–5] at explaining the exotic electronic properties of cuprates, in particular, the origin of the so-called pseudogap region, involve quantum critical fluctuations of orbital currents (OCs). These currents have been suggested to flow in the elementary O-Cu-O plaquettes within the  $CuO_2$  planes and break time-reversal symmetry. Whether the translational invariance is violated depends on the suggested current pattern. The distinguishing characteristic of the formation of any such pattern is the resulting magnetic-field distribution.

So far, there is no agreement on the actual current path nor on its strength. Various experimental attempts to assess the orbital-current models have been made and provide evidence for breaking of time-reversal symmetry from observations of dichroism in angle-resolved photoemission spectroscopy (ARPES) measurements on  $Bi_2Sr_2CaCu_2O_{8+\delta}$  [6]. However, it is possible that the observed effect is caused by superlattice modulations [7]. Introduction of Pb removes these structural distortions. Subsequent ARPES measurements on samples without this superstructure did not reveal any dichroism [8]. Translational symmetry is expected to be broken for the *d*-density wave (DDW) phase [1,3], since the corresponding unit cell doubles. In contrast to the DDW phase, a scenario of circulating currents (CCs) [5] preserves the translational symmetry. Recently reported neutron data [9] show qualitative consistency with one of the proposed patterns of CCs. The observed unusual long-range magnetic order in the pseudogap region of  $YBa_2Cu_3O_{6+x}$  is

static on the time scale of neutron scattering experiments, and the reported moments are of considerable strength ( $0.05$ – $0.1 \mu_B$ ). A very recent zero-field muon-spin rotation experiment [10] on  $La_{2-x}Sr_xCuO_4$  provides a rather low upper limit for static time-reversal violating local fields of 0.02 mT. However, according to Ref. [11] the magnetic field at the muon site, expected to be of several mT, is reduced by more than 2 orders of magnitude due to muon-related screening and finite-stiffness effects of the order parameter.

To our knowledge, there are no reports in the literature on a nuclear magnetic resonance (NMR) study dealing directly with current patterns confined to the copper plaquette in cuprates. NMR is a highly suitable method for studying magnetic fields using the noninvasive nuclear moments of the compounds' own atoms as microscopic probes. While NMR gives information on static as well as fluctuating internal fields, its ability to directly test the orbital-current models depends on the proposed current path and strength. Static fields arising from the proposed current phases (DDW and CC) cannot be seen directly in NMR measurements on nuclei of ions located in the  $CuO_2$  plane, since the fields cancel at these sites for symmetry reasons. In YBCO compounds, the Y ions do not lie at centers of symmetry for the DDW and the CC phases, when considering just a single plane. As  $^{89}Y$  is experimentally accessible through NMR,  $^{89}Y$  NMR experiments should be sensitive to OC effects. Lee and Sha proposed such NMR measurements in the cuprate superconductor  $Y_2Ba_4Cu_7O_{15-\delta}$  (Y247) [12]. This specific material exhibits a high transition temperature to superconductivity of  $T_c = 95$  K and shows a clear pseudogap phase above  $T_c$  [13]. It consists of alternating  $YBa_2Cu_3O_{7-\delta}$  (Y123) and  $YBa_2Cu_4O_8$  (Y124) blocks. Pure Y124 is in the underdoped regime, featuring a pronounced pseudogap, whereas pure Y123 is close to optimal doping, showing no pseudogap features above  $T_c$ . The main structural difference

between Y123 and Y124 is that the latter possesses double chains with no oxygen vacancy, in contrast to single-chain Y123. As in Y124 and Y123, the  $\text{CuO}_2$  planes in Y247 form bilayers separated by Y ions. Unlike the parent compounds, the adjacent planes in Y247 are unequally doped [13]. As was pointed out by Lee and Sha, this doping difference should to some extent prevent a possible cancellation of the staggered magnetic fields between bilayers [12].

In this Letter, we address the presence of OCs in Y247 by means of  $^{89}\text{Y}$  NMR. With this method, and using the relation  $^{89}\omega_L = ^{89}\gamma_n B$  ( $^{89}\gamma_n$  is the gyromagnetic ratio of the  $^{89}\text{Y}$  nucleus) connecting the Larmor frequency  $\omega_L$  with the magnetic field  $B$ , we are able to monitor the local magnetic field at the single Y site accurately. Since  $^{89}\text{Y}$  carries no quadrupole moment, the measured NMR linewidth (LW) and the nuclear spin-lattice relaxation (NSLR) are of purely magnetic origin. In our experiment, the observed field  $B$  is the sum of a large externally applied magnetic field  $B_0$  and much smaller internal magnetic fields, part of the latter possibly stemming from OCs. Since the pseudogap is insensitive to large external magnetic fields [14], we conclude that  $B_0$  should have a minor, if any, effect on the orbital currents. Note that if the internal fields are much smaller than  $B_0$ , then, in general, the internal static magnetic fields influence the NMR LW only when pointing along  $B_0$ . For the NSLR process of  $^{89}\text{Y}$ , only magnetic fields fluctuating in a direction perpendicular to  $B_0$  are relevant. We provide upper limits for static and dynamic field amplitudes created at the Y site in the normal-conducting phase.

The Y247 sample was prepared using solid-state techniques described elsewhere [15]. A pure Y247 phase with a phase-impurity level of less than 0.5% by volume was achieved. The powder was suspended in epoxy and oriented in a 9 T field in order to study anisotropic properties. This procedure yields samples with a high degree of  $c$ -axis alignment of its grains, whereas the  $a$  and  $b$  axes of the crystallites remain randomly distributed.

The NMR experiments were performed using a conventional phase-coherent pulse NMR spectrometer with an external field of  $B_0 = 9$  T. The  $^{89}\text{Y}$  NMR spectra were obtained by complex Fourier transformation of the spin echoes, which were recorded using a phase-alternating spin-echo accumulation technique. The NSLR time  $T_1$  was measured using a saturation-pulse sequence. Temperatures in the range from 310 down to 100 K were controlled with a precision of better than 0.1 K.

Now we describe and discuss our results concerning static field effects originating from possible OCs. The formation of a static DDW or CC pattern in a plane, expected at  $T_c < T < 310$  K, leads to a magnetic-field arrangement exhibiting additional static fields at the Y site. Because of the planar confinement of the currents, these fields are either directed perpendicular to the  $\text{CuO}_2$  planes or lie parallel to them, depending on the type of

pattern. In the case of CCs, the fields at all of the Y sites in a domain of correlated currents point in the same direction parallel to the plane. However, with  $B_0$  applied parallel to the planes ( $B_0 \perp c$ ), a symmetric broadening of the Y line, and not a shift, is expected for the following reasons: (i) The  $a$ - and  $b$ -axis directions of the crystallites in the  $c$ -axis-oriented powder are randomly distributed in a plane perpendicular to the  $c$  axis, and (ii) the domains of correlated CCs are of finite size. The DDW scenario, on the other hand, leads to antiferromagnetically arranged fields at neighboring Y sites within a particular domain, pointing perpendicular to the  $\text{CuO}_2$  planes. Hence, a splitting of the absorption line should be observed when  $B_0$  is applied perpendicular to the planes ( $B_0 \parallel c$ ). However, this splitting may well be unresolved. In this case, an additional symmetric broadening of the Y line should still appear. Thus the temperature dependence of the  $^{89}\text{Y}$  LW is directly influenced by the appearance of OCs, but in the discussed cases only for a particular direction of  $B_0$ .

The temperature dependence of the  $^{89}\text{Y}$  NMR LW and frequency in the normal-conducting phase of Y247 from

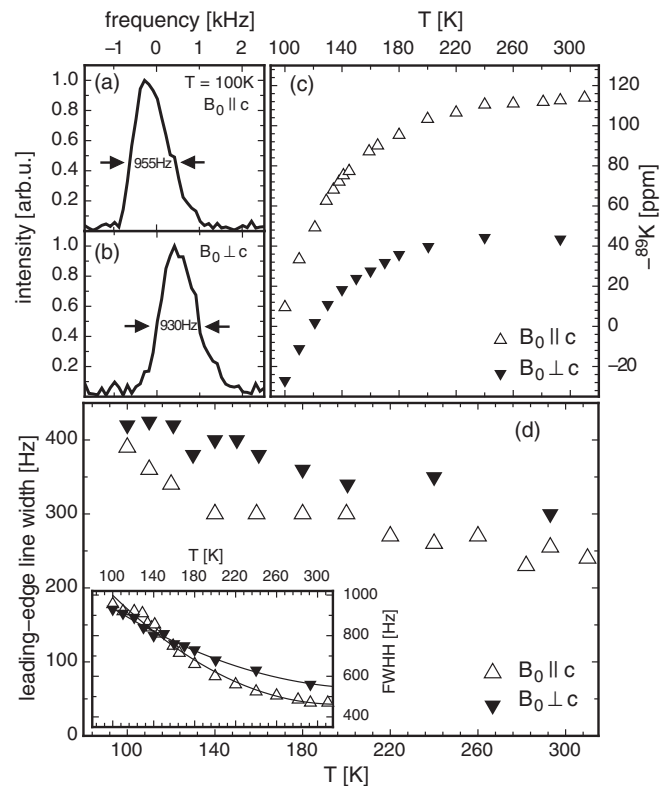


FIG. 1.  $^{89}\text{Y}$  NMR data measured in  $B_0 = 9$  T for field orientations parallel ( $\parallel$ ) and perpendicular ( $\perp$ ) to the crystalline  $c$  axis in oriented powder of  $\text{Y}_2\text{Ba}_4\text{Cu}_7\text{O}_{15-\delta}$ . Panels (a) and (b) show typical absorption lines relative to 18.867 53 MHz at 100 K for both field orientations with a FWHH of 955(50) and 930 (50) kHz, respectively. Panel (c) displays the temperature dependence of the magnetic shift. In (d), the temperature dependence of the leading-edge  $^{89}\text{Y}$  NMR linewidth at half height is shown. The inset shows the temperature dependence of the FWHH (solid lines are guides to the eye).

room temperature down to 100 K were measured for both field orientations. The results are presented in Fig. 1. When cooling, a substantial drop of the measured  $^{89}\text{Y}$  magnetic shift [Fig. 1(c)] was observed, which clearly demonstrates the presence of the pseudogap state in the sample. Figures 1(a) and 1(b) display typical examples of the measured  $^{89}\text{Y}$  absorption lines at 100 K for both field orientations. In pure Y124, we obtained a Y absorption line, which has a symmetric shape for all temperatures from room temperature down to 100 K with a nearly constant width. This behavior implies that the Y LW of stoichiometric Y124 is mainly due to dipolar interactions. In contrast, Y247 exhibits an Y line asymmetry towards higher frequencies, which we attribute to doping inhomogeneity of the Y247 compound introduced by the Y123 blocks. It is known that in this temperature range the non-stoichiometric Y123 compounds exhibit oxygen clustering in the CuO chains which affects the homogeneity of the doping. The magnetic shift is strongly dependent on the mobile carrier density (doping). Thus, a variation in carrier density entails a distribution of the Y magnetic shift, leading to a broadening of the Y line. The magnetic line shift of Y arises mainly from two contributions: a negative carrier-related shift and a positive temperature-independent chemical shift [16]. Oxygen clustering in the single chains causes a carrier-density variation, which cannot exceed the density of Y1237 (filled chains, slightly overdoped) but can have values corresponding to substantial underdoping. Since the Y magnetic shift is negative, the broadening of the Y line is asymmetric towards higher frequencies. Upon cooling from room temperature, the Y magnetic shift decreases when the pseudogap opens [Fig. 1(c)]; the larger the magnitude of the pseudogap, the stronger the decrease. The magnitude of the pseudogap strongly depends on the doping level. Nearly optimally doped Y123 shows almost no temperature dependence of the plane copper shift, whereas underdoped Y124 with its substantial pseudogap shows a strong decrease of the plane copper shift in the investigated temperature range (see, e.g., Ref. [13]). Therefore, inhomogeneous doping should lead to a steady increase of the full Y LW in Y247, accompanied by a growing asymmetry of the line shape with decreasing temperature. This is indeed observed. The full Y LW (FWHH) [Fig. 1(d), inset] and its skewness increase for both field orientations when cooling. In addition, we detect a crossing of the two temperature dependences of the FWHH at  $\sim 140$  K. This is expected from doping inhomogeneity, since for measurements with  $B_0 \parallel c$  the drop of the magnetic shift due to the pseudogap is more pronounced as compared to the one with  $B_0 \perp c$  [Fig. 1(c)]. This difference causes a stronger line broadening for  $B_0 \parallel c$  than  $B_0 \perp c$ , implying that the two curves for  $B_0 \parallel c$  and  $B_0 \perp c$  cross each other at  $\sim 140$  K [Fig. 1(d), inset].

In order to minimize the disturbing influence of doping inhomogeneity, we have focused on the leading-edge LW at half height (LEW) to detect the symmetric broadening due to possible OCs. The temperature dependence of the

LEW for both field orientations is plotted in Fig. 1(d). The high-temperature limit of the LEW for Y247 agrees with that of Y124, within measurement uncertainties. For both field orientations at 100 K, an increase in the LEW of  $\sim 150$  Hz is obtained as compared to the 310 K value. Assuming this increase is caused entirely by static OC effects, the maximum field amplitude at the Y site in Y247 is  $[\{(400 \text{ Hz})^2 - (250 \text{ Hz})^2\}/^{89}\gamma_n^2]^{(1/2)} \approx 0.15$  mT. This number was deduced under the conservative assumption that different effects contributing to the LEW add quadratically. Note that the LEW increases for both field orientations.

A bilayer structure possibly causes a cancellation of fields if there is an antiferromagnetic interplane interaction between OCs of neighboring planes. Although results from neutron measurements favor an in-phase OC circulation [9,17], we assume antiphase circulation because of the coupling between OCs from adjacent planes, which increases the upper limit of the single plane field. The carrier density in Y247 for planes from both blocks (Y123 and Y124) has been deduced, and a difference of  $\sim 20\%$  was determined [13]. We take the difference of the orbital-current strength  $j$  to be of the same order of magnitude, because  $j$  is inversely proportional to the doping level [4,18]. Therefore, in the case of antiphase circulation of OCs in neighboring planes, we may have to increase our single layer limit by a factor of  $\sim 5$  and end up with a maximum field of  $\sim 0.75$  mT at the Y site from OCs in a single  $\text{CuO}_2$  plane. Unless the actual current pattern differs from the proposed ones, a LW broadening due to OCs is expected only for one orientation, which is not the case. Therefore, the estimated field amplitude due to OCs is rather strongly exaggerated.

Next, we describe and discuss the NSLR and LW experiments in the context of possible nonstatic OCs and provide an upper limit for the additional field amplitude at the Y site due to fluctuating OCs. For the NSLR rate  $1/T_1$ , the time-dependent local magnetic fields perpendicular to the quantization axis, given by  $B_0$ , are relevant. As stated before, OCs create fields that fluctuate either parallel or perpendicular to the  $\text{CuO}_2$  planes. Consequently, the appearance of fluctuating OCs on varying the temperature should change the rate anisotropy  $R = {}^{89}T_1^{\parallel}/{}^{89}T_1^{\perp}$ .  ${}^{89}T_1^{\parallel}$  ( ${}^{89}T_1^{\perp}$ ) denotes the relaxation time for  $B_0$  parallel (perpendicular) to the  $c$  axis. The NSLR rate in the normal-conducting phase has been determined up to 300 K for both field orientations. The  $^{89}\text{Y}$  magnetization relaxation shows the expected single-exponential relaxation behavior. At 100 K, we found  ${}^{89}T_1^{\parallel} = 103.4(2.0)$  s and  ${}^{89}T_1^{\perp} = 91.0(2.5)$  s. The measured NSLR rate can be written as a sum  $1/{}^{89}T_1 = 1/{}^{89}T_1' + 1/{}^{89}T_1^{\text{orb}}$ , where the first term in the sum is the rate due to mechanisms not related to OCs and the second term is due to possible OCs. Within error, the measured  $R$  is constant from 100 to 300 K with a weighted average of  $\bar{R} = 1.145(18)$ . Taking twice the error of  $\bar{R}$  as the upper limit of the change due to possible OCs at

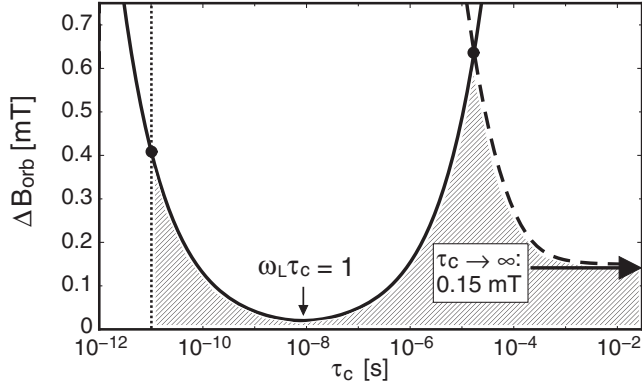


FIG. 2. Dependence of the possible OC field amplitude  $\Delta B_{\text{orb}}$  on the OC correlation time  $\tau_c$  from  $^{89}\text{Y}$  NSLR measurements in Y247 at 100 K (solid line, see text). The lower limit of  $\tau_c$  from neutron (dotted line) and the upper limit of  $\tau_c$  from LW measurements (dashed line) are shown. The shaded area represents all  $\Delta B_{\text{orb}}$  consistent with the  $^{89}\text{Y}$  LW and NSLR measurements. The horizontal arrow indicates the maximum static field  $\leq 0.15$  mT.

100 K, the maximum effect at the lowest temperature measured does not exceed 3%. Considering this possible change as being caused purely by fluctuating OCs, we deduce an upper limit for the corresponding fluctuating field amplitude. The relation between  $^{89}\text{T}_1^{\text{orb}}$ , the fluctuating OC field amplitude  $\Delta B_{\text{orb}}$ , and the associated correlation time for the fluctuating orbital-current pattern  $\tau_c$  is given by [19]

$$\frac{1}{^{89}\text{T}_1^{\text{orb}}} \approx \frac{^{89}\gamma_n^2 \Delta B_{\text{orb}}^2}{1 + (\omega_L \tau_c)^2} \tau_c. \quad (1)$$

Taking an additional contribution of 3% for the NSLR rate due to possible OCs (see above) and  $\Delta B_{\text{orb}} = \{[1 + (\omega_L \tau_c)^2]/(^{89}\gamma_n^2 T_1^{\text{orb}} \tau_c)\}^{(1/2)}$  from Eq. (1), we plot  $\Delta B_{\text{orb}}$  versus  $\tau_c$  (see solid line in Fig. 2). To get an upper limit for  $\Delta B_{\text{orb}}$ , we restrict  $\tau_c$  at high and low frequency. In the fast fluctuation regime, the lower limit  $\tau_c > 10^{-11}$  s is given by a recent neutron measurement on YBCO [9] (see dotted line in Fig. 2) [20]. To determine an upper boundary for  $\tau_c$ , we use the result of the LW measurement and apply the formula for LW motional narrowing [21]

$$\delta\omega^2 = \delta\omega_r^2 + (\delta\omega_{\text{static}}^{\text{orb}})^2 \frac{2}{\pi} \arctan(\alpha \delta\omega \tau_c), \quad (2)$$

where  $\delta\omega$  denotes the motionally narrowed LW,  $\delta\omega_{\text{static}}^{\text{orb}}$  represents the LW broadened by static orbital-current effects only,  $\delta\omega_r$  is the LW at high temperatures, where the fast fluctuating orbital-current effects on the LW are averaged out, and  $\alpha$  is a dimensionless factor of the order of unity. Reformulating Eq. (2) and using  $\delta\omega_{\text{static}}^{\text{orb}} = 2 \times ^{89}\gamma_n \Delta B_{\text{orb}}$  (the factor of 2 is due to the two possible field directions) yields  $\Delta B_{\text{orb}} = \frac{1}{2^{89}\gamma_n} [(\delta\omega^2 - \delta\omega_r^2) \frac{\pi}{2} / \arctan(\alpha \tau_c \delta\omega)]^{(1/2)}$ . Taking twice the measured high-temperature LEW of 250 Hz [Fig. 1(d)] as  $\delta\omega_r/2\pi$  and twice the LEW of 400 Hz at 100 K as  $\delta\omega/2\pi$ , we are able

to plot the corresponding  $\Delta B_{\text{orb}}$  as a function of  $\tau_c$  (dashed line in Fig. 2). From Fig. 2, it is obvious that  $^{89}\text{Y}$  NMR experiments set an upper limit for the OC field amplitude at the Y site in Y247 of  $\Delta B_{\text{orb}} \leq 0.7$  mT at 100 K. In the case that this field is the result of putative antiphase circulating OCs in the neighboring planes, then, as discussed before, the limit for the field coming from one plane only would have to be increased by a factor of  $\sim 5$ .

In summary, from our  $^{89}\text{Y}$  NMR measurements in  $\text{Y}_2\text{Ba}_4\text{Cu}_7\text{O}_{15-\delta}$  we conclude that any additional static magnetic field at the Y site, showing up in the normal-conducting state below room temperature, is smaller than 0.15 mT. For the fluctuating field amplitude, we find an upper limit  $\leq 0.7$  mT. These values are considerably smaller than theoretical predictions for YBCO, which are in the range of several tens of mT; see, e.g., [11].

The authors appreciate discussion with M. V. Eremin, P. F. Meier, and B. Graneli. Financial support by the Swiss National Foundation is acknowledged.

\*simon.straessle@physik.uzh.ch

- [1] T. C. Hsu, J. B. Marston, and I. Affleck, Phys. Rev. B **43**, 2866 (1991).
- [2] C. Nayak, Phys. Rev. B **62**, 4880 (2000).
- [3] S. Chakravarty, R. B. Laughlin, D. K. Morr, and C. Nayak, Phys. Rev. B **63**, 094503 (2001).
- [4] C. M. Varma, Phys. Rev. B **73**, 155113 (2006).
- [5] V. Aji and C. M. Varma, Phys. Rev. Lett. **99**, 067003 (2007).
- [6] A. Kaminski *et al.*, Nature (London) **416**, 610 (2002).
- [7] J. P. Castellan *et al.*, Phys. Rev. B **73**, 174505 (2006).
- [8] S. V. Borisenko *et al.*, Phys. Rev. Lett. **92**, 207001 (2004).
- [9] B. Fauqué *et al.*, Phys. Rev. Lett. **96**, 197001 (2006).
- [10] G. J. MacDougall *et al.*, arXiv:0801.2716.
- [11] Arkady Shekhter *et al.*, arXiv:0802.2972.
- [12] P. A. Lee and G. Sha, Solid State Commun. **126**, 71 (2003).
- [13] R. Stern *et al.*, Phys. Rev. B **50**, 426 (1994).
- [14] K. Gorny *et al.*, Phys. Rev. Lett. **82**, 177 (1999); Guo-qing Zheng *et al.*, Phys. Rev. B **60**, R9947 (1999).
- [15] J.-Y. Genoud *et al.*, Physica (Amsterdam) **192C**, 137 (1992).
- [16] H. Alloul, T. Ohno, and P. Mendels, Phys. Rev. Lett. **63**, 1700 (1989).
- [17] Y. Sidis *et al.*, Physica (Amsterdam) **397B**, 1 (2007).
- [18] M. V. Eremin, I. Eremin, and A. Terzi, Phys. Rev. B **66**, 104524 (2002).
- [19] C. P. Slichter, *Principles of Magnetic Resonance* (Springer, Berlin, 1990).
- [20] Since the orbital-current phase is thought of as a thermodynamic state with a well-defined transition, the energy scale of involved fluctuations must be well below the transition temperature to stabilize the phase. Considering this, energy arguments also end up with a correlation time similar to the one from neutron measurements.
- [21] A. Abragam, *Principles of Nuclear Magnetism* (Clarendon, Oxford, 1961).